The Journal of Microbiology (2010) Vol. 48, No. 2, pp. 174-183
DOI 10.1007/s12275-010-9199-5

Experimental and Computational Characterization of the Ferric Uptake Regulator from *Aliivibrio salmonicida* (*Vibrio salmonicida*)

Hege Lynum Pedersen[1], Rafi Ahmad[1], Ellen Kristin Riise[2,3], Hanna-Kirsti Schrøder Leiros[2], Stefan Hauglid[2], Sigrun Espelid[1,2†], Bjørn Olav Brandsdal[2,3,4], Ingar Leiros[2,3], Nils-Peder Willassen[1,2], and Peik Haugen[1,2*]

[1]*Department of Molecular Biotechnology, Institute of Medical Biology, Faculty of Medicine, University of Tromsø, N-9037, Norway*
[2]*The Norwegian Structural Biology Centre, University of Tromsø, N-9037, Norway*
[3]*Department of Chemistry, Faculty of Science, University of Tromsø, N-9037, Norway*
[4]*The Centre for Theoretical and Computational Chemistry, University of Tromsø, N-9037, Norway*

(Received July 2, 2009 / Accepted September 17, 2009)

The Ferric uptake regulator (Fur) is a global transcription factor that affects expression of bacterial genes in an iron-dependent fashion. Although the Fur protein and its iron-responsive regulon are well studied, there are still important questions that remain to be answered. For example, the consensus Fur binding site also known as the "Fur box" is under debate, and it is still unclear which Fur residues directly interact with the DNA. Our long-term goal is to dissect the biological roles of Fur in the development of the disease cold-water vibriosis, which is caused by the psychrophilic bacteria *Aliivibrio salmonicida* (also known as *Vibrio salmonicida*). Here, we have used experimental and computational methods to characterise the Fur protein from *A. salmonicida* (AS-Fur). Electrophoretic mobility shift assays show that AS-Fur binds to the recently proposed vibrio Fur box consensus in addition to nine promoter regions that contain Fur boxes. Binding appears to be dependent on the number of Fur boxes, and the predicted "strength" of Fur boxes. Finally, structure modeling and molecular dynamics simulations provide new insights into potential AS-Fur–DNA interactions.

***Keywords*:** ferric uptake regulator, Fur, iron homeostasis, *A. salmonicida*, *V. salmonicida*

The biochemical properties of *Escherichia coli* Fur (EC-Fur) and its role in iron homeostasis have been studied for almost three decades (Hantke, 1981), and homologs from multiple bacteria (e.g., *Pseudomonas*, *Vibrio*, *Salmonella*, *Yersinia*, *Neisseria*, *Listeria*, and *Bacillus*) have been described. When the intracellular level of iron is high the Fur protein complexes with Fe^{2+} and will, in most cases, act as a repressor (for exceptions see Delany *et al*., 2004; Lee *et al*., 2007). Fur-Fe^{2+} dimers will bind to specific Fur binding sites (called Fur boxes) in promoter regions and reduce transcription of the associated genes. The "classical" Fur box is a 19 nt palindromic sequence centered on an A or T (de Lorenzo *et al*., 1987). Recently, several consensus sequences from different bacteria have been suggested, and they usually differ from the "classical" Fur box by being centered on a degenerate nucleotide (*N*), which is positioned 3 nt downstream relative to the A/T center nucleotide in the classical *E. coli* Fur box. For example, the vibrio Fur box consensus (5′-AATGANAAT*N*ATTNTCATT-3′) (Ahmad *et al*., 2009b) is nearly identical to that of *Bacillus subtilis* (Fuangthong and Helmann, 2003) and *Yersinia pestis* (Zhou *et al*., 2006; Gao *et al*., 2008). Moreover, Schneider and coworkers (Chen *et al*., 2007) recently used computer-based methods to search for Fur boxes in *E. coli*, *B. subtilis*, and *P. aeruginosa*, and found that they are highly similar and positioned 3 nt downstream relative to the "classical" *E. coli* Fur box. Intriguingly, under low iron conditions the *Vibrio vulnificus* Fur protein can bind with low affinity to a 37-nt sequence in the *fur* promoter region and positively regulate Fur expression (Lee *et al*., 2007). It is unknown how the Fur protein interacts with this sequence, but the central 15-nt of the sequence strongly resembles the central part of the vibrio Fur box (TGCAAAT*T*GTTATTA and TGANAAT*N*ATTNTCA, respectively) (center of pseudo-palindrome is shown in italic).

Genes that are differentially expressed in an iron-dependent manner have been mapped in wild-type and/or *fur* mutants (e.g., Stojiljkovic *et al*., 1994; Baichoo *et al*., 2002; Grifantini *et al*., 2003; Mey *et al*., 2005b; Zhou *et al*., 2006; Gao *et al*., 2008), and include genes important for acquisition and storage of iron, oxidative stress, and other stress responses, metabolism, chemotaxis, motility, in addition to a number of genes with unknown function. Importantly, Fur also regulates expression of *ryhB*, which encode the RyhB regulatory small RNA (Massé and Gottesmann, 2002; Mey *et al*., 2005a). When expressed, RyhB partially base-pairs with a subset of mRNAs and target these for degradation (Massé *et al*., 2003). Because *ryhB* is negatively regulated by Fur, the RyhB mRNA targets are apparently positively regulated by Fur under high iron concentrations, i.e., when the Fur-Fe^{2+} complex is repressing RyhB expression.

Three crystal structures of Fur have been solved, i.e., a structure of Fur from *Pseudomonas aeruginosa* (PA-Fur) (Pohl

† Deceased author. * For correspondence. E-mail: peik.haugen@uit.no; Tel: +47-7764-5288; Fax: +47-7764-5350

et al., 2003), a structure of the N-terminal DNA-binding domain of *E. coli* Fur (EC-Fur) (Pecqueur *et al*., 2006), and a near complete (i.e., no electron density map of the last 17 amino acids) structure of *Vibrio cholerae* Fur (VC-Fur) (Sheikh and Taylor, 2009). The structures are similar, although some differences can be noted, i.e., in the metal binding sites. For example, in VC-Fur and PA-Fur a Zn^{2+} in the dimerization domain (Zn1) appears to be tetra- and hexa-coordinated, respectively (see Sheikh and Taylor, 2009). The Fur protein functions as a homodimer, in which each monomer apparently contains one Zn^{2+} and one Fe^{2+} binding site, and consists of one N-terminal DNA-binding domain (residues 1-83 in PA-Fur) and one C-terminal dimerization domain (residues 84-135 in PA-Fur). The DNA-binding domain has four helices in front of two anti-parallel beta-strands, and exhibits a winged helix fold. In a PA-Fur–DNA structure model helix 4 was implicated in DNA binding, and in EC-Fur a tyrosine residue (Tyr 56) in helix 4 is in direct contact with the DNA target, and is in close proximity with two thymines (pos. 15 and 16) in the Fur binding site (Tiss *et al*., 2005). By using computer-based methods we recently showed that several other Fur residues (e.g., K13, R18, R56, R69, Q60, and H76) might also significantly contribute to Fur-DNA interactions (Ahmad *et al*., 2009a).

Aliivibrio salmonicida (formerly *Vibrio salmonicida*) is a psychrophilic and moderately halophilic marine bacteria, and is the causative agent of cold-water vibriosis. The complete genome sequence of *A. salmonicida* strain LFI1238 was recently published (Hjerde *et al*., 2008). It encodes a temperature-dependent siderophore-based iron sequestration system (see Colquhoun and Sørum, 2001), three *tonB* systems that provide energy for uptake of iron, and a Fur protein. We recently predicted Fur binding sites on a global scale for available *Aliivibrio/Vibrio* genomes, and found 60 single genes and 20 operons that are potentially Fur-regulated in *A. salmonicida* (Ahmad *et al*., 2009b). In this current work we characterised basic properties of Fur from *A. salmonicida* (AS-Fur). The *fur* gene was cloned, over-expressed and purified, and AS-Fur–DNA interaction was studied using EMSA and computer-based methods. Our data provide further insights into the correlation between Fur-binding, and the number/"strength" of Fur boxes. Also, we identified new Fur residues and Fur box nucleotides that might be directly involved in protein-DNA interactions.

Materials and Methods

Cloning, expression and purification of AS-Fur

The *fur* gene from *A. salmonicida* was PCR-amplified and cloned into the pDEST14 Gateway expression vector according to the manufacturers instructions (Invitrogen, USA). AS-Fur was expressed in *E. coli* BL21(DE3) cells and was grown in LB broth with 100 μg/ml ampicillin. Over-expression was initiated from the T7 promoter at OD_{600}=0.6 by adding 0.5 mM Isopropyl β-D-1-thiogalactopyranoside (IPTG) (Promega, USA) at 20°C, and grown over night. Finally, cells were harvested by centrifugation at 5,000×g for 30 min at 4°C and resuspended in lysis buffer (25 mM Tris-HCl; pH 8.0, 1 M NaCl, 1 mM EDTA) to an OD_{600} of about 35. The solution was stored at -20°C, or kept at 4°C, depending on when the subsequent purification steps were done. Next, 1 tablet EDTA-free proteinase inhibitors (Roche, Swizerland) was added and the cells were disrupted by sonication using a Vibracell ultrasonic processor VCX 750 (Sonics and Materials). Sonication settings were 9.9 sec on and 9.9 sec off for 45 min, maximum allowed temperature in solution was set to 20°C, and 40% intensity. After sonication the crude extract was centrifuged at 25,000×g for 30 min at 4°C to separate the recombinant protein from the majority of cell debris. The AS-Fur protein was affinity purified by running the supernatant on a 5 ml His-trap column (GE Healthcare, UK) using the Äkta FPLC (GE Healthcare) at 4°C. Buffer A (50 mM Tris-HCl; pH 8.0, 1 M NaCl, 5 mM β-mercaptoethanol and 1% glycerol) was used as the running buffer and the flow rate was set at 1.0 ml per min. AS-Fur was finally eluted with buffer B (Buffer A+500 mM Imidazole) by collecting 5 ml fractions and measuring the optical density at 280 nm. Fractions containing AS-Fur were collected and loaded on a Superdex 200 10/300 gel filtration column (GE Healthcare) equilibrated with 50 mM Tris-HCl (pH 8.0), 200 mM NaCl, 5 mM β-mercaptoethanol, and 1% glycerol, and the flow rate set at 0.4 ml/min. Fractions containing AS-Fur protein were pooled. AS-Fur was concentrated using an Amicon Ultra-4 spin column with cut-off of 5,000 Da (Millipore, USA). AS-Fur was unstable under our storage conditions and typically aggregated within 5-7 days. New batches of AS-Fur were therefore freshly made before experiments. The final yield of AS-Fur was measured using a spectrophotometer with the wavelength of 280 nm and the theoretical extinction coefficient of AS-Fur.

Electrophoretic gel mobility shift assay (EMSA)

Radio-labelled PCR products of 80 bp or 194-245 bp were used as DNA probes. These were amplified in standard PCR reactions using synthetic oligonucleotides or *A. salmonicida* genomic DNA as template, respectively. To ensure equal amounts of labeled DNA target in each EMSA reaction the DNA targets were prepared as follows: DNA targets were PCR-amplified from 250 ng templates using 10 μM of "cold" upstream primer and 10 μM [γ-^{32}P] end-labeled downstream primer. PCR products were subsequently purified using QIAquick Nucleotide Removal kit (QIAGEN, Germany) to remove unincorporated nucleotides and primers. Finally, 10,000 cpm of PCR product was used in each reaction. As an extra control, PCR products were run on agarose gels and stained with Ethidium bromide to ensure equal amounts of DNA.

Synthetic oligonucleotide templates 5′-GGTGATCAGTGTGGA AATGATAATAATTATCATTTGCGTAGTGGGAGTG-3′ ("consensus"), 5′-GGTGATCAGTGTGGAAATGAGAATGGTTATTATTTGCGTAG TGGGAGTG-3′ (RyhB-1), 5′-GGTGATCAGTGTGGAGTTGAGAT TAGATCTCATTGCGTAGTGGGAGTG-3′ (RyhB-2) and 5′-GGTG ATCAGTGTGGATATCTTATTGATAATTAATGCGTAGTGGGAG TG-3′ (RyhB-3) contained the Fur box (underlined) flanked by sequences that are unfavorable for Fur binding. PCR products were amplified from these oligonucleotides with primer pair *fwd* (5′-GTAAA ACGACGGCCAGGTGATCAGTGTGGA-3′) and *rev* (5′-CAGGAA ACAGCTATGACACTCCCACTACGCA-3′).

Gene promoters from *A. salmonicida* were PCR-amplified using primers 5′-TGTGACGTAGATCTATTTTTACAAACC-3′ and 5′-AAG TTGACGAGGCCACTTTAG-3′ (VSAL_I2118, formerly TVS 2098), 5′-TTTTTCATCAAAGTATTGAGCACT-3′ and 5′-AAGCAAAGAA AGCGCAAAAA-3′ (VSAL_II0868, formerly TVS4378), 5′-ATATCC CTGCTCCCCAAAAT-3′ and 5′-TCTGCATCGATTTCTTGTGC-3′ (VSAL_I0833, formerly TVS0690), 5′-GCGTAACGCTAGATTTGAG TTC-3′ and 5′-TTCCAATATTATGTGAAACCACAC-3′ (VSAL_p320_ 27, formerly pVS320_0029), 5′-TCCTATATAAAGTAATTCAGCCTGT

GA-3′ and 5′-CGCGATGGTTATTTTCCACT-3′ (VSAL_I1951, formerly TVS1921), 5′-GGATGAATGCCTTCTTTCATTT-3′ and 5′-AAACGA GGTTGACGAGGAAC-3′ (VSAL_I0891, formerly TVS0751), 5′-GGACGTTAATTCGTCCCTTTT-3′ and 5′-TTCTTGTGCTCTAGG AGATAGGG-3′ (VSAL_I1342, formerly TVS1251), and 5′-ATCC AAAACAAAAGCGCATC-3′ and 5′-TTGTTCGCCAAAAGTCTTCA-3′ (VSAL_I1864, formerly TVS1829).

Purified AS-Fur was incubated for 20 min in binding buffer containing 20 mM Tris acetate, pH 8.0, 1 mM $MgCl_2$, 50 mM KCl, 1 mM DTT, 50 ng polyD(AT), and 100 µM $MnCl_2$. Thereafter, labeled DNA (10,000 cpm) was mixed with the desired concentration of AS-Fur and incubated for another 10 min before the reaction was loaded on the gel. Samples were run on native 6% polyacrylamide/1× TB gels at 200 V for 2-2 1/2 h at 6°C with circulating buffer. The gel was finally dried and exposed to a phosphor imaging screen (Fujifilm, Japan). The phosphor imaging screen was scanned using a BAS-5000 phosphoimager (Fujifilm), and the ImageGauge v4.0 software was used to analyse the results.

Computational details

A homology model of AS-Fur was built using the crystal structures of PA-Fur (1MZB, shares ca. 56% sequence identity to AS-Fur) and EC-Fur (2FU4, shares ca. 80% sequence identity to AS-Fur in the DNA-binding domain) as templates, with the help of the Modeller software (Sali and Blundell, 1993). Superimposition of the modeled AS-Fur with PA-Fur and EC-Fur gives a root mean square deviation (RMSD) of 1 and 0.8 Å, respectively. After finishing our computer analyses the crystal structure of VC-Fur, which was solved at 2.6 Å resolution by molecular replacement methods based on the PA-Fur structure, was published (Sheikh and Taylor, 2009). The structures of the individual domains of PA- and VC-Fur are very similar, with a slightly different orientation of the DNA-binding domains. Even so, we wanted to evaluate if knowledge on the VC-Fur structure would significantly change our results. We therefore superimposed the monomers A and B of VC-Fur with the corresponding monomers of AS-Fur. The resulting RMSD values were 2.2 and 1.9 Å, respectively, which indicate that the structures of the individual domains are highly similar. Also, the DNA-binding and dimerization domains of AS-Fur and VC-Fur were superimposed and resulted in RMSD values of 0.4 and 0.7 Å, respectively. In summary, based on our superimpositions we conclude that the modeled AS-Fur structure, which is based on the PA-Fur structure, is highly similar to the recently published VC-Fur, and our analyses with the modeled AS-Fur should therefore be valid.

The vibrio-specific Fur box (5′-AATGATAATAATTATCATT-3′) and a control sequence (i.e., the sequence with the least conserved nucleotide at each position; 5′-CCGTGCGCACTCCGCAGGG-3′) were next manually docked separately to the AS-Fur protein model. Docking was done based on the recently published PA-Fur–DNA model (Ahmad *et al*., 2009a). Molecular dynamics (MD) simulations and binding free energy calculations were performed as previously described (Ahmad *et al*., 2009a). Briefly, MD simulations on the AS-Fur–DNA complex (with bound Fe^{2+} at site 2) were done using the AMBER 9 simulation package (Case *et al*., 2008), and the molecular mechanics-Poisson-Boltzmann surface area (MM-PBSA) and molecular mechanics-generalised Born surface area methods (MM-GBSA) were used to calculate the binding energy and the per-residue free energy decomposition of the protein-DNA complex, respectively.

To examine the stability of the simulations RMSD of backbone atoms versus simulation time was calculated. RMSD was calculated relative to the first structure from the production phase, and the result showed that structures were stable throughout the MD simulations (Fig. 1). In addition, the total energy, temperature, pressure, volume, and density deviations were plotted against time, and all these properties were stable throughout the simulations (data not shown). Finally, to evaluate the stability (or convergence) of the computed free energies, we plotted the sum of the gas phase energies and the solvation free energy for the AS-Fur-DNA complex extracted from MD simulations, stable energies with fluctuation within 2% of the mean value were observed (Fig. 2).

Results and Discussion

Basic properties of Fur from members of the *Vibrionaceae* family

The Fur protein is highly conserved within the *Vibrionaceae* family (gamma-proteobacteria), which is dominated by different groups of vibrios (Fig. 3). Vibrio Fur proteins are 54-58% identical to the PA-Fur, and encode an additional 12-15 amino acids at the C-terminal end (similar to EC-Fur). The optional C-terminal tail has been associated with metal binding, folding

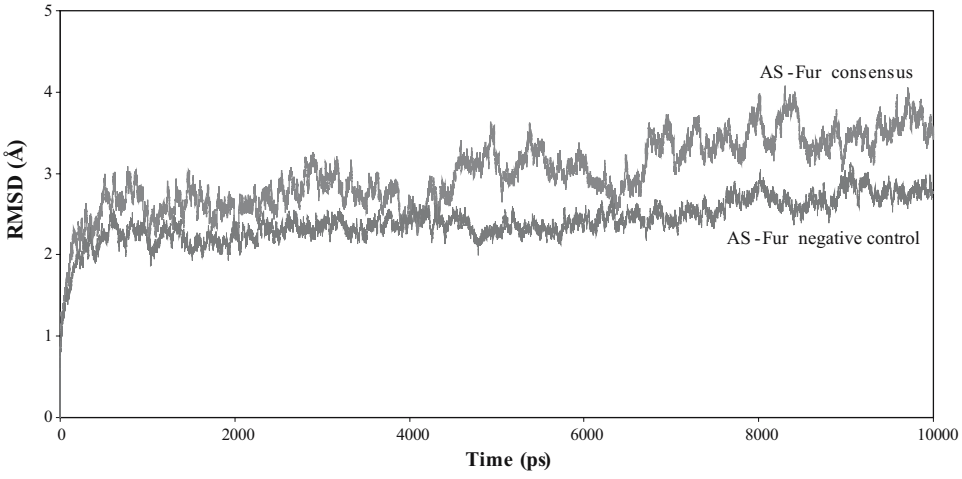

Fig. 1. RMSD plot of AS-Fur consensus and AS-Fur negative control as a function of time for MD simulations.

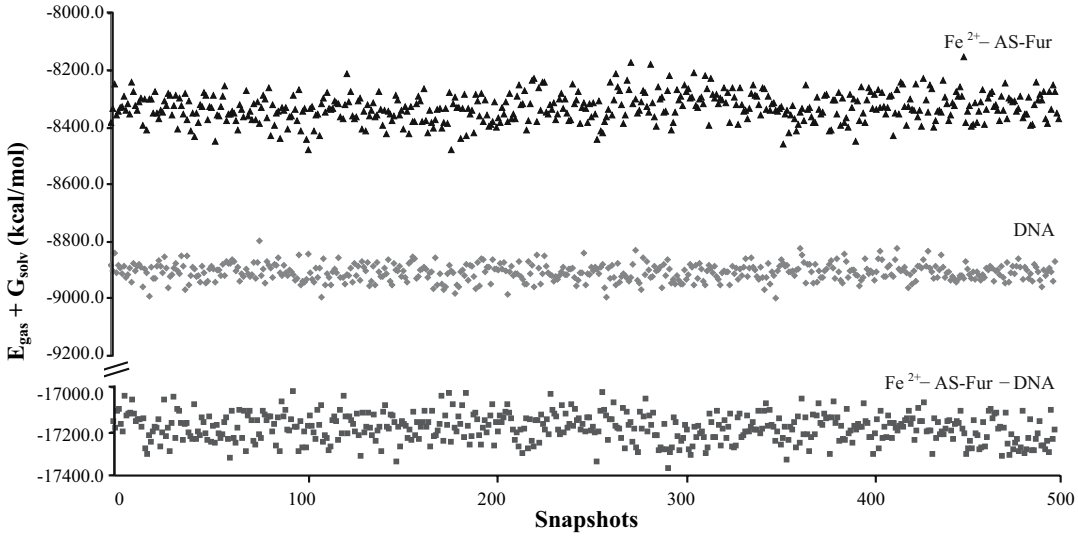

Fig. 2. Plot of the sum of gas phase energies and the solvation free energy for MD simulations.

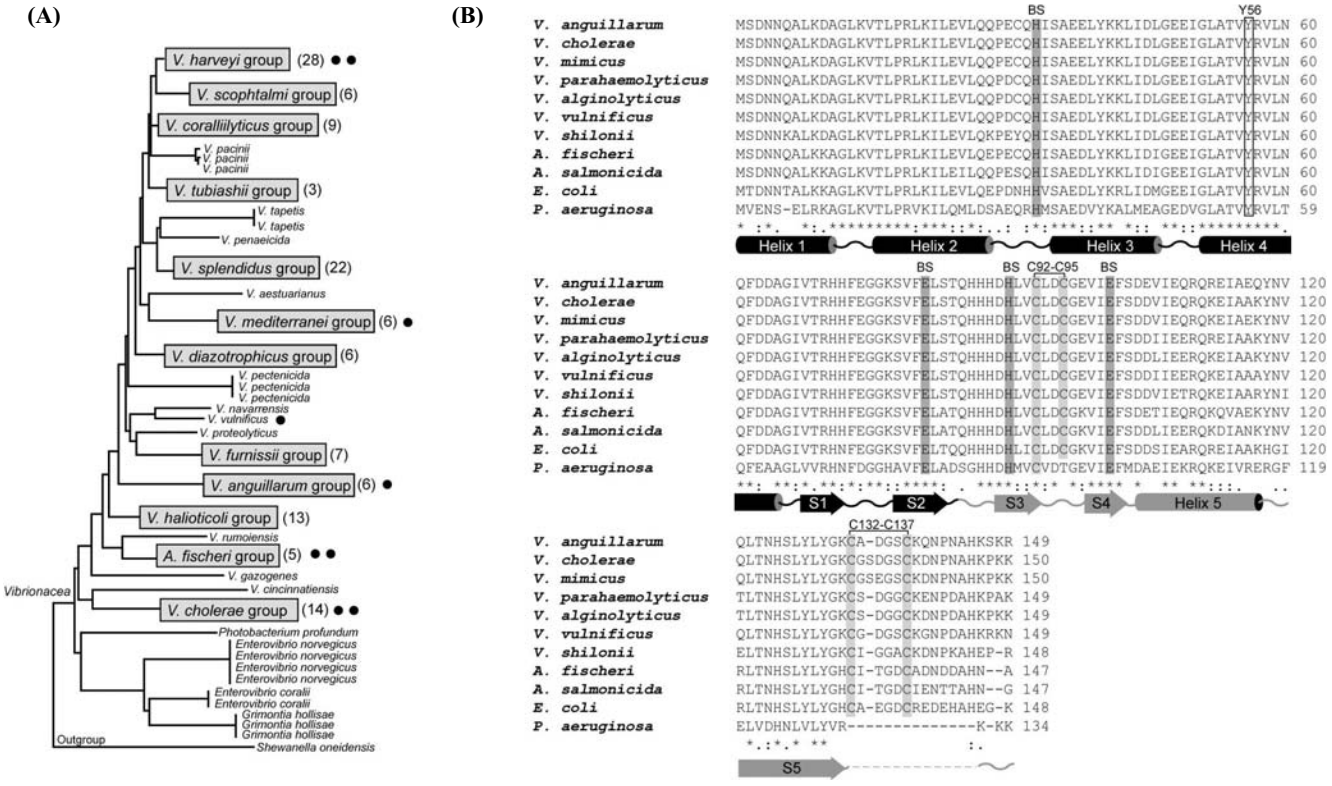

Fig. 3. Basic properties of Fur from the *Vibrionaceae* family. (A) Summary of phylogenetic tree by Thompson and co-workers (Thompson *et al*., 2007) based on the *atpA* gene showing evolutionary relationships between representatives of the *Vibrionaceae* family. The majority of representatives are different species of vibrios. The *Aliivibrio fischeri* group is the formerly *V. fischeri* group which includes *A. salmonicida*. Numbers in parentheses denote the number of sequences included in the analysis. Filled circles denote groups that are represented in the Fur sequence alignment (B). (B) Secondary structure elements for PA-Fur as deduced from the crystal structure (Pohl *et al*., 2003) are shown. BS, potential binding site residues for iron; Y56, tyrosine 56 which is in direct contact with DNA target (Tiss *et al*., 2005); C92-C95 and C132-C135, cysteine residues involved in disulfide bridge formation in *E. coli* (D'Autréaux *et al*., 2007). At each position an asterisk indicates identical residues, a colon denotes conserved substitutions, and a dot represents semi-conserved substitutions.

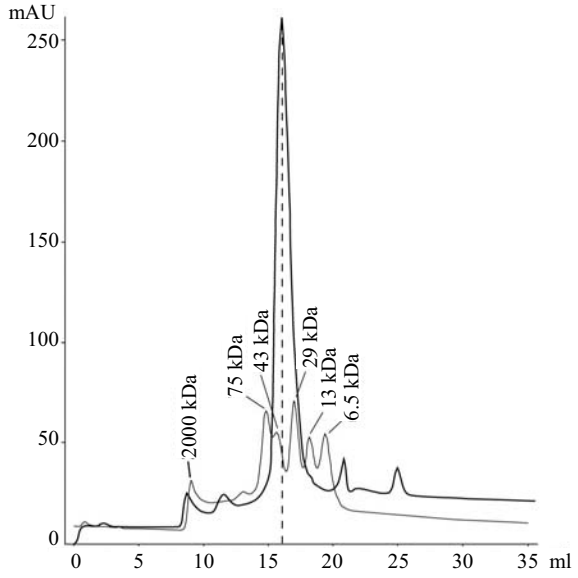

Fig. 4. Gel filtration of AS-Fur. The gel filtration chromatogram shows that the purified AS-Fur protein has a molecular weight of ~40 kDa in solution, which is consistent with an AS-Fur homodimer (38 kDa).

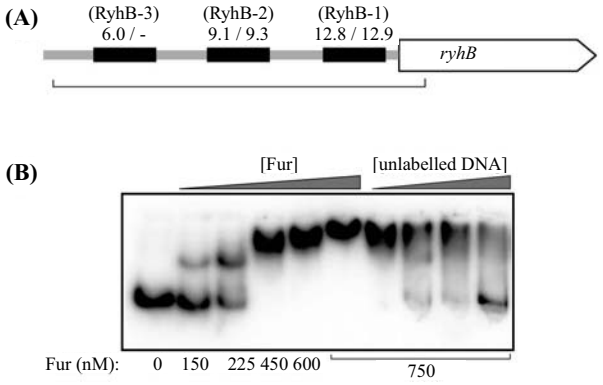

Fig. 5. EMSA using AS-Fur and the *ryhB* promoter. (A) Schematic drawing of the *A. salmonicida ryhB* gene. The promoter contains three Fur boxes, named RyhB-1, RyhB-2, and RyhB-3. (B) Autoradiogram showing AS-Fur binding to radio-labelled *ryhB* promoter. Increasing concentrations (0.5-4 fold) of unlabelled DNA was added as competitor DNA.

activation and dimerization (Pecqueur *et al*., 2006), and contains two cysteine residues (C^{132} and C^{137} in *E. coli*), which in *E. coli* form a disulfide bridge in their oxidised state (D'Autréaux *et al*., 2007). Interestingly, C^{132} in the *Vibrio alginolyticus* Fur protein appears to be inessential as it can be replaced without significant changes to the activity of the protein (Liu *et al*., 2007), and the last 12 residues of the Fur protein from the closely related *Vibrio harveyi* (Fig. 3A) can be deleted without loss of protein function (Sun *et al*., 2008). The *A. salmonicida fur* encodes a protein of 147 amino acids (i.e., AS-Fur) with a theoretical pI of 5.75 and a theoretical molecular weight of 16.6 kDa. AS-Fur is 83% identical to the *V. cholerae* Fur and 79% identical to EC-Fur. Differences in primary sequence of the compared Fur proteins are primarily located at the C-terminal end (Fig. 3B). Finally, residues important for direct interaction with DNA (Y^{56}; Tiss *et al*., 2005), metal binding (H^{33}, E^{81}, H^{90}, and E^{100}; Pohl *et al*., 2003), and disulfide bridge formation (C^{93} and C^{96}, C^{133} and C^{138}; Pecqueur *et al*., 2006; D'Autréaux *et al*., 2007) are conserved in all vibrios and aliivibrios.

DNA binding of *A. salmonicida* Fur

To study DNA binding of AS-Fur, the corresponding gene from *A. salmonicida* was cloned into a Gateway vector for over-expression in *E. coli*. Expression produced AS-Fur, which was purified to apparent homogeneity. The subsequent gel filtration analysis revealed that the protein mainly exists as a homodimer in solution (Fig. 4). Purified AS-Fur and a radio-labeled DNA target was next used in an electrophoretic mobility shift assay (EMSA) to test for AS-Fur–DNA complex formation. A 250 nt PCR-amplified fragment from the promoter region of *ryhB* (encodes the RyhB sRNA) was used as the DNA target. The *A. salmonicida ryhB* promoter region contains three predicted Fur boxes immediately upstream of the sRNA-encoding sequence (Fig. 5A), and expression of RyhB is highly dependent on iron (Ahmad *et al*., 2009b). Interestingly, instead of changing the promoter mobility to a single slow-moving band, the EMSA analysis showed that AS-Fur is responsible for gradually decreasing promoter mobility as AS-Fur concentrations increases (Fig. 5B). This gel retardation pattern is consistent with an increasing number of AS-Fur on the DNA, and is in agreement with earlier studies that showed Fur polymerization on specific DNA sequences (Le Cam *et al*., 1994). Furthermore, specificity of DNA binding was shown by adding increasing amounts of unlabeled *ryhB* promoter DNA (i.e., competitor DNA) to the binding reaction, which resulted in increasing mobility of the radio-labeled target. In contrast, addition of a similar-sized DNA fragment with no Fur box (i.e., non-competitor DNA) did not alter the EMSA profile (data not shown).

Binding of AS-Fur to promoters correlates with the iron responsiveness of genes and the "strength" of Fur boxes

In a previous study, we predicted Fur boxes in front of 60 single genes and 20 operons in the *A. salmonicida* genome, and tested previously unrecognised Fur-regulated genes and operons (7 genes and 2 operons) for iron responsiveness using Northern blot analysis (Ahmad *et al*., 2009b). In this current study we PCR-amplified the nine previously tested promoters and run EMSA. Figure 6A shows the resulting phosphoimage scan, schematic drawings of each promoter (which include predicted Fur boxes), and the iron responsiveness of the genes. In general, DNA binding correlates well with the iron responsiveness of genes and the "strength" of predicted Fur boxes. For example, the four strongest mobility shifts correspond to those genes that are most responsive to iron (i.e., 16.5-8.3 fold change), and they all contain two or three predicted Fur boxes. Furthermore, at least one Fur box in each promoter has a high (12-16) or medium (8-11) Patser score. High Patser scores indicate high probability for Fur-binding.

All tested promoters contain at least two Fur boxes, and it is

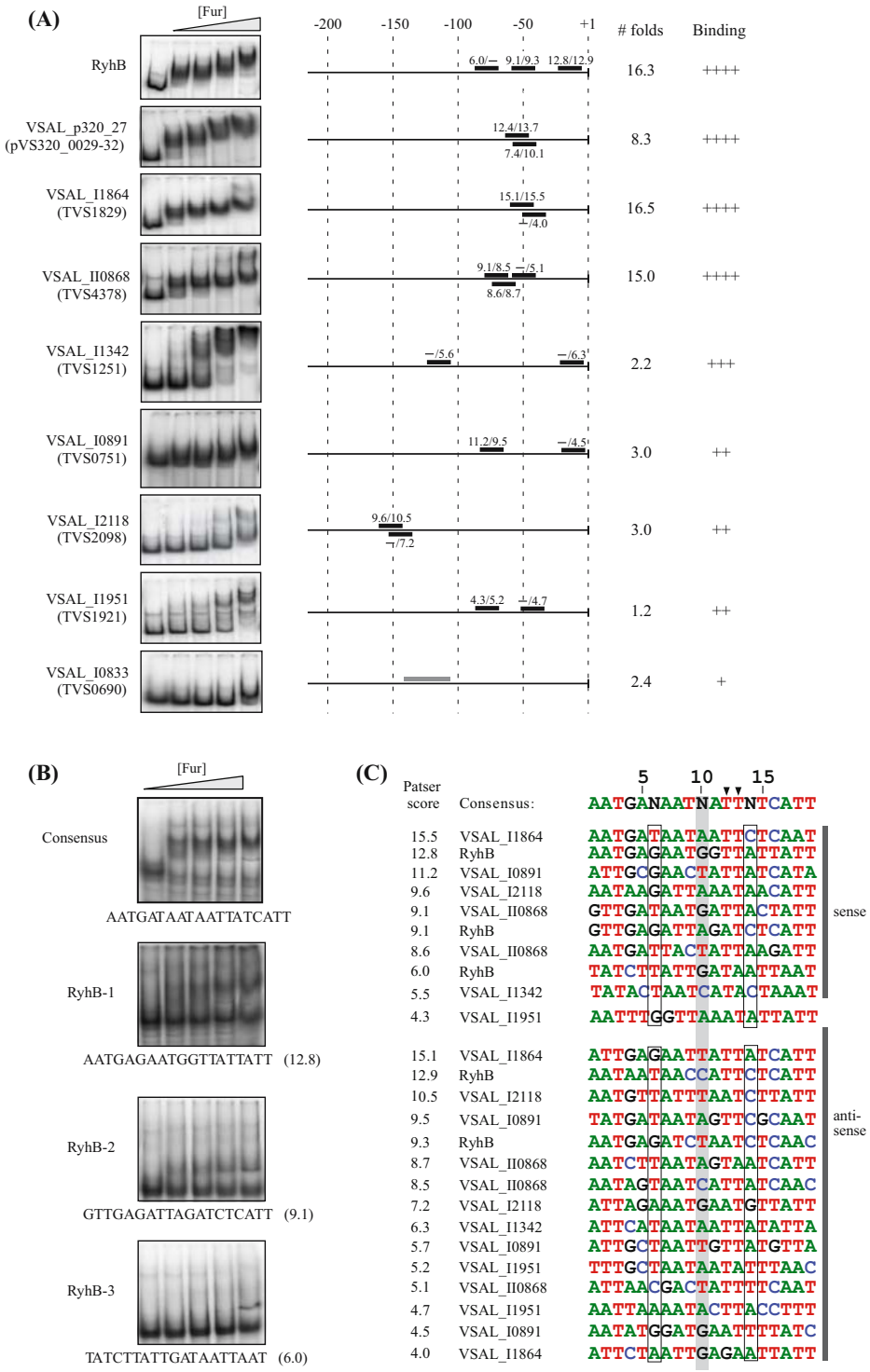

Fig. 6. EMSA using AS-Fur and promoter DNA. (A) Increasing concentrations of AS-Fur (0 nM, 150 nM, 225 nM, 450 nM, and 900 nM) was added to nine radio-labelled PCR-amplified promoters. The associated genes are expressed in an iron-dependent fashion (Ahmad *et al*., 2009b), and fold change of expression during iron-poor conditions compared to standard conditions is indicated. Binding of AS-Fur to DNA targets were categorised as strong (++++), good (+++), weak (++) or poor (+). Patser scores of individual Fur boxes are shown. Values to the left are for Fur boxes in sense orientation and values to the right are for Fur boxes in anti-sense orientation. The first nucleotide in the translation start codon is defined as position +1. (B) Autoradiogram showing AS-Fur–binding to the vibrio "consensus" sequence and individual Fur boxes from the *ryhB* promoter (RyhB-1, RyhB-2, and RyhB-3). The DNA targets were 80 nt in length and were PCR-amplified from synthetic DNA templates (see 'Material and Methods' for details). Sequences of each Fur box in sense orientation, and the associated Patser score for RyhB-1, RyhB-2, and RyhB-3 are shown. (C) Sequence alignment of all Fur boxes shown in (A) and (B). Sequence from sense and anti-sense orientations are shown.

Table 1. Binding free energies for AS-Fur–DNA complexes

Molecular model	ΔE_{elec}	ΔE_{vdW}	ΔE_{int}	ΔG_{np}	ΔG_{pol}	$\Delta G_{gas+solv}$	$T\Delta S_{tot}$	ΔG_{tot}
AS-Fur–DNA (vibrio Fur-box)	2410.36 (5.5)	-124.46 (0.3)	0 (0)	-20 (0.1)	-2343.35 (5.1)	-77.46 (0.6)	-71.25 (0.8)	-6.21 (1.4)
AS-Fur–DNA (neg. control)	2886.14 (9.9)	-125.02 (0.4)	0 (0)	-20.05 (0.1)	-2762.42 (9.4)	-21.35 (0.6)	-88.66 (0.8)	67.31 (1.4)

Binding free energy values were computed from MM-PBSA single trajectories. Values are in kcal/mol. Numbers in parentheses are standard errors of the mean and were calculated by dividing the standard deviation by the square-root of the number of snapshots (500). E_{elec}, Coulombic energy; E_{vdW}, van der Waals energy; E_{int}, internal energy; G_{np}, non-polar salvation free energy; G_{pol}, polar solvation free energy; $G_{gas+solv} = E_{elec} + E_{vdW} + E_{int} + G_{np} + G_{pol}$; TS_{tot}, Total entropic contributions; $G_{tot} = G_{gas+solv} - TS_{tot}$.

possible that AS-Fur binds to these cooperatively. To test Fur boxes individually we produced shorter PCR products (approx. 80 bp in length), which contained one single Fur box flanked by sequences that are unfavorable for AS-Fur binding. The vibrio Fur box "consensus" (5′-AATGATAATAATTATCATT-3′) and three Fur boxes from the *ryhB* promoter, with Patser scores 12.8/12.9, 9.1/9.3 or 6.0/– ("–" denotes below threshold value), were PCR-amplified and tested for AS-Fur binding using EMSA (Fig. 6B). First, the results show that AS-Fur produces a strong shift in complex with the "consensus" target. However, mobility shifts do not increase with higher concentrations of AS-Fur, which suggests that AS-Fur does not aggregate on the DNA maybe because the DNA is only 80 nt in length, and contains only one Fur box. Second, the results show correlation between the Patser score of the individual *ryhB*-associated Fur boxes and the mobility shifts, i.e., higher Patser score is associated with stronger shift. This is perhaps not surprising because the Patser score value is based on similarity to the vibrio Fur box consensus sequence (Fig. 6C). Even so it demonstrates the usefulness of using computer predictions to search for transcription factor binding sites.

Binding free energy for AS-Fur–DNA complex

Our EMSA results show that AS-Fur recognizes and binds to the proposed vibrio-specific Fur box consensus, and that binding of AS-Fur to promoters correlates, in general, with the responsiveness of genes to iron and the strength of predicted Fur boxes. Next, we used MD simulations to approximate the strength of AS-Fur–DNA interactions, and to predict amino acid and nucleotide residues that significantly contribute to this interaction. MD simulations were performed using the AS-Fur (with ferrous iron at metal site 2) in complex with the vibrio Fur box "consensus" or the "anti-consensus" (negative control) DNA. Binding free energies were calculated using the MM-PBSA method (Srinivasan *et al*., 1998; Kollman *et al*., 2000). The binding energy values were calculated to -6.21 and 67.31 kcal/mol, respectively (Table 1). The former value is similar to that calculated for PA-Fur in complex with the *E. coli* "classical" Fur box and Fe^{2+} at metal site 2 (-8.9 kcal/mol) (Ahmad *et al*., 2009a), whereas the latter value strongly support that the AS-Fur– "anti-consensus" complex is unfavorable. In summary, our calculations suggest that the AS-Fur protein recognizes the vibrio Fur box specifically and that it binds with strong affinity.

AS-Fur residues potentially involved in interaction with the DNA

By calculating the contribution of individual residues to the overall binding free energy, we next predicted potential AS-Fur residues that directly interact with the DNA (the vibrio "consensus", 5′-AATGATAATAATTATCATT-3′). Figure 7 shows that a number of amino acid residues contribute signifycantly to the overall binding free energy of the AS-Fur–DNA interaction. The majority of contributing residues overlap with those predicted in our recent study, in which the PA-Fur was used in complex with the *E. coli* Fur box (Ahmad *et al*., 2009a). However, a number of contributing residues are specific to AS-Fur, including K42, N60, H72, S78, K98, K117, and R121, whereas a few contributing residues (R31, R115, and R117) are specific to PA-Fur. PA-Fur significantly differs from vibrio

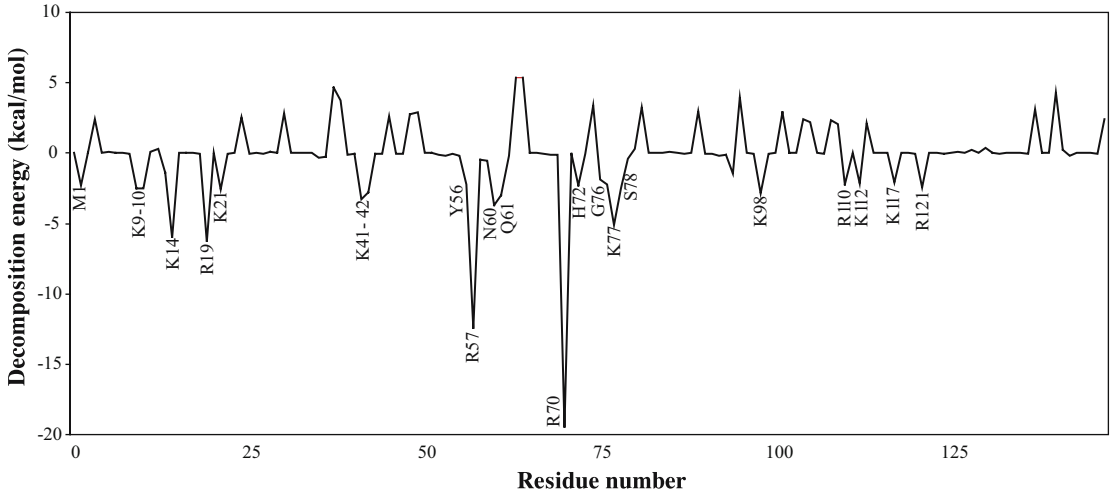

Fig. 7. Free energy of binding per residue for AS-Fur, in complex with vibrio "consensus" Fur box. Based on the calculations, residues contributing significantly to Fur-DNA interaction are highlighted.

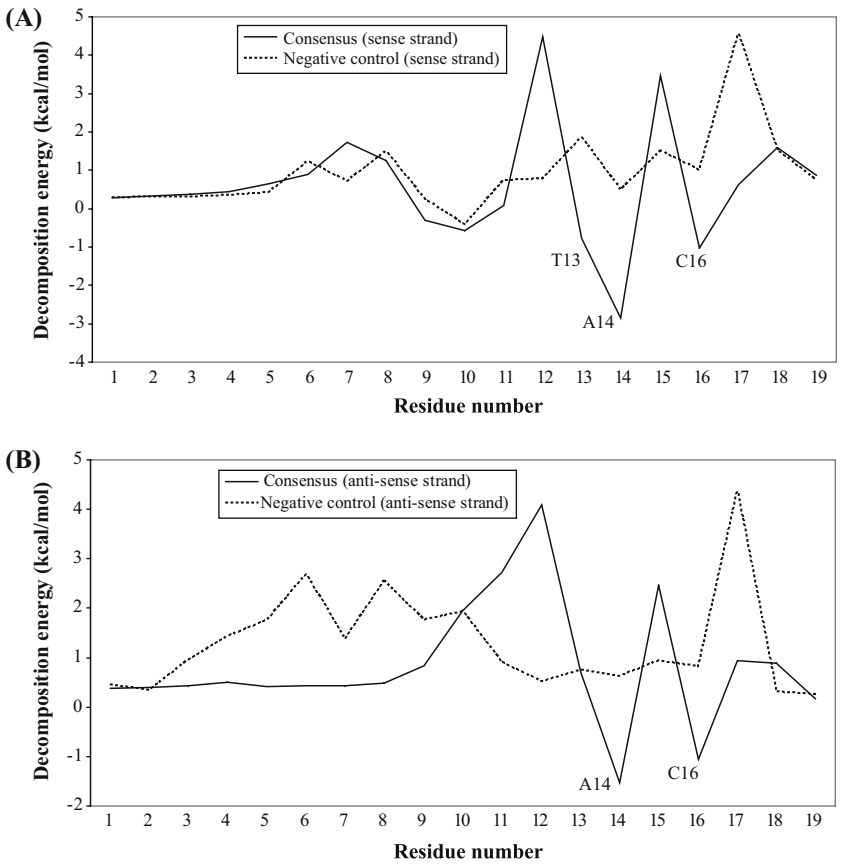

Fig. 8. Free energy of binding per residue for vibrio "consensus" Fur box, in complex with AS-Fur. (A) Per-residue binding free energy decomposition for sense strand of vibrio Fur box "consensus" and negative control. (B) Per-residue binding free energy decomposition for anti-sense strand of vibrio Fur box "consensus" and negative control. Highlighted DNA residues contribute favorably to the free energy of binding for AS-Fur and the vibrio Fur box.

Fur proteins in sequence composition (approx. 56% identity between PA-Fur and AS-Fur), and some species-specific interactions between Fur and DNA can therefore be expected.

Vibrio-specific Fur box residues involved in interaction with AS-Fur

Using the same approach as described above, contribution of individual nucleotide residues to the overall binding free energy in the AS-Fur–vibrio Fur box complex was calculated. Figure 8 shows that A14 and C16 (correspond to A17 and C19 in *E. coli*) contribute favorably to the interaction on both strands, whereas T13 (T16 in *E. coli*) was found to contribute to binding on one strand. It is unclear to us if the strand-specific contribution of T13 is due to real differences in interactions between the DNA and the Fur homodimer, or if it is due to an artifact in the MD simulations and binding free energy calculations. Using a mass spectrometry-based method, EC-Fur and the *E. coli* "classical" Fur box, Tiss and co-workers (Tiss *et al*., 2005) showed that T12 and T13 (correspond to T15 and T16 in *E. coli*) directly interact with the protein. In summary, A14 and C16, which are conserved in *B. subtilis* and *Y. pestis*, represent new potential interaction sites between Fur and DNA. A structure presentation of potential interactions between AS-Fur and the vibrio "consensus" DNA

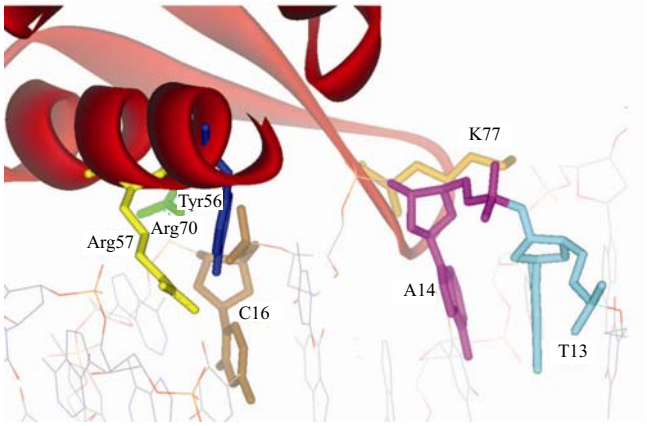

Fig. 9. Ribbon presentation of potential interactions between AS-Fur and the target DNA. The presented structure was chosen as the complex with the average overall energy during the last 4 ns of MD simulations. Highlighted DNA and amino acid residues contribute significantly to the free energy of binding for AS-Fur and the vibrio Fur box (see Figs. 8 and 9). For the sake of clarity only a selected amino acids residues have been highlighted. The figure was made using the Accelrys Discovery Studio Visualizer software.

is shown in Fig. 9, and indicates that the C16 nucleotide and the Tyr56, Arg57 and Arg70 amino acids are in close proximity.

Conclusions

Knowledge on Fur from different bacterial species is continuously increasing. As a result species-specific functions of Fur also accumulate. Our model system is the Gram-negative bacterium *A. salmonicida*, which is responsible for cold-water vibriosis in Atlantic salmon and cod. It is our goal to elucidate the roles of Fur during the development of this disease. Previously, we have employed computational methods to establish the *Vibrionaceae* Fur box and used this information to predict Fur binding sites in *A. salmonicida*, and used experimental methods to verify the iron responsiveness of a set of genes. In this study we used EMSA to show Fur-binding to the proposed Fur box, as well as to several other promoters of proposed Fur-regulated genes. Finally, we performed MD simulations and binding free energy calculations to evaluate AS-Fur–DNA interactions and to predict important nucleotides and amino acid residues possibly involved in AS-Fur–DNA binding.

Acknowledgements

This work was supported by The University of Tromsø, the Norwegian Research Council and The National Programme for Research and Functional Genomics in Norway (FUGE). The Norwegian Structural Biology Centre (NorStruct) is supported by a grant from FUGE.

References

Ahmad, R., B.O. Brandsdal, I. Michaud-Soret, and N.P. Willassen. 2009a. Ferric uptake regulator protein: Binding free energy calculations and per-residue free energy decomposition. *Proteins* 75, 373-386.

Ahmad, R., E. Hjerde, G.Å. Hansen, P. Haugen, and N.P. Willassen. 2009b. Prediction and experimental testing of ferric uptake regulator regulons in vibrios. *J. Mol. Microbiol. Biotechnol*. 16, 159-168.

Baichoo, N., T. Wang, R. Ye, and J.D. Helmann. 2002. Global analysis of the *Bacillus subtilis* Fur regulon and the iron starvation stimulon. *Mol. Microbiol.* 45, 1613-1629.

Case, D.A., T.A. Darden, T.E. Cheatham, 3rd, C.L. Simmerling, J. Wang, R.E. Duke, R. Luo, and *et al*. 2008. AMBER 10, University of California, San Francisco, USA.

Chen, Z., K.A. Lewis, R.K. Shultzaberger, I.G. Lyakhov, M. Zheng, B. Doan, G. Storz, and T.D. Schneider. 2007. Discovery of Fur binding site clusters in *Escherichia coli* by information theory models. *Nucleic Acids Res.* 35, 6762-6777.

Colquhoun, D.J. and H. Sørum. 2001. Temperature dependent siderophore production in *Vibrio salmonicida*. *Microb. Pathog.* 31, 213-219.

D'Autréaux, B., L. Pecqueur, A. Gonzalez de Peredo, R.E. Diederix, C. Caux-Thang, L. Tabet, B. Bersch, E. Forest, and I. Michaud-Soret. 2007. Reversible redox- and zinc-dependent dimerization of the *Escherichia coli* fur protein. *Biochemistry* 46, 1329-1342.

de Lorenzo, V., S. Wee, M. Herrero, and J.B. Neilands. 1987. Operator sequences of the aerobactin operon of plasmid ColV-K30 binding the ferric uptake regulation (fur) repressor. *J. Bacteriol.* 169, 2624-2630.

Delany, I., R. Rappuoli, and V. Scarlato. 2004. Fur functions as an activator and as a repressor of putative virulence genes in *Neisseria meningitidis*. *Mol. Microbiol.* 52, 1081-1090.

Fuangthong, M. and J.D. Helmann. 2003. Recognition of DNA by three ferric uptake regulator (Fur) homologs in *Bacillus subtilis*. *J. Bacteriol.* 185, 6348-6357.

Gao, H., D. Zhou, Y. Li, Z. Guo, Y. Han, Y. Song, J. Zhai, Z. Du, X. Wang, J. Lu, and R. Yang. 2008. The iron-responsive Fur regulon in *Yersinia pestis*. *J. Bacteriol.* 190, 3063-3075.

Grifantini, R., S. Sebastian, E. Frigimelica, M. Draghi, E. Bartolini, A. Muzzi, R. Rappuoli, G. Grandi, and C.A. Genco. 2003. Identification of iron-activated and -repressed Fur-dependent genes by transcriptome analysis of *Neisseria meningitidis* group B. *Proc. Natl. Acad. Sci. USA* 100, 9542-9547.

Hantke, K. 1981. Regulation of ferric iron transport in *Escherichia coli* K12: isolation of a constitutive mutant. *Mol. Gen. Genet.* 182, 288-292.

Hjerde, E., M.S. Lorentzen, M.T. Holden, K. Seeger, S. Paulsen, N. Bason, C. Churcher, and *et al*. 2008. The genome sequence of the fish pathogen *Aliivibrio salmonicida* strain LFI1238 shows extensive evidence of gene decay. *BMC Genomics* 9, 616.

Kollman, P.A., I. Massova, C. Reyes, B. Kuhn, S. Huo, L. Chong, M. Lee, and *et al*. 2000. Calculating structures and free energies of complex molecules: combining molecular mechanics and continuum models. *Acc. Chem. Res.* 33, 889-897.

Le Cam, E., D. Frechon, M. Barray, A. Fourcade, and E. Delain. 1994. Observation of binding and polymerization of Fur repressor onto operator-containing DNA with electron and atomic force microscopes. *Proc. Natl. Acad. Sci. USA* 91, 11816-11820.

Lee, H.J., S.H. Bang, K.H. Lee, and S.J. Park. 2007. Positive regulation of *fur* gene expression via direct interaction of Fur in a pathogenic bacterium, *Vibrio vulnificus*. *J. Bacteriol.* 189, 2629-2636.

Liu, Q., P. Wang, Y. Ma, and Y. Zhang. 2007. Characterization of the *Vibrio alginolyticus fur* gene and localization of essential amino acid sites in fur by site-directed mutagenesis. *J. Mol. Microbiol. Biotechnol.* 13, 15-21.

Massé, E., F.E. Escorcia, and S. Gottesman. 2003. Coupled degradation of a small regulatory RNA and its mRNA targets in *Escherichia coli*. *Genes Dev.* 17, 2374-2383.

Massé, E. and S. Gottesman. 2002. A small RNA regulates the expression of genes involved in iron metabolism in *Escherichia coli*. *Proc. Natl. Acad. Sci. USA* 99, 4620-4625.

Mey, A.R., S.A. Craig, and S.M. Payne. 2005a. Characterization of *Vibrio cholerae* RyhB: the RyhB regulon and role of *ryhB* in biofilm formation. *Infect. Immun.* 73, 5706-5719.

Mey, A.R., E.E. Wyckoff, V. Kanukurthy, C.R. Fisher, and S.M. Payne. 2005b. Iron and Fur regulation in *Vibrio cholerae* and the role of Fur in virulence. *Infect. Immun.* 73, 8167-8178.

Pecqueur, L., B. D'Autréaux, J. Dupuy, Y. Nicolet, L. Jacquamet, B. Brutscher, I. Michaud-Soret, and B. Bersch. 2006. Structural changes of *Escherichia coli* ferric uptake regulator during metal-dependent dimerization and activation explored by NMR and X-ray crystallography. *J. Biol. Chem.* 281, 21286-21295.

Pohl, E., J.C. Haller, A. Mijovilovich, W. Meyer-Klaucke, E. Garman, and M.L. Vasil. 2003. Architecture of a protein central to iron homeostasis: crystal structure and spectroscopic analysis of the ferric uptake regulator. *Mol. Microbiol.* 47, 903-915.

Sali, A. and T.L. Blundell. 1993. Comparative protein modelling by satisfaction of spatial restraints. *J. Mol. Biol.* 234, 779-815.

Sheikh, A. and G.L. Taylor. 2009. Crystal structure of the *Vibrio cholerae* ferric uptake regulator (Fur) reveals insights into metal co-ordination. *Mol. Microbiol*. 75, 1208-1220.

Srinivasan, J., T.E. Cheatham, 3rd, P. Cieplak, P.A. Kollman, and D.A. Case. 1998. Continuum solvent studies of the stability of DNA, RNA, and phosphoramidate-DNA helices. *J. Am. Chem. Soc.* 120, 9401-9409.

Stojiljkovic, I., A.J. Bäumler, and K. Hantke. 1994. Fur regulon in

Gram-negative bacteria. Identification and characterization of new iron-regulated *Escherichia coli* genes by a fur titration assay. *J. Mol. Biol.* 236, 531-545. Erratum in: *J. Mol. Biol.* 1994. 240, 271.

Sun, K., S. Cheng, M. Zhang, F. Wang, and L. Sun. 2008. Cys-92, Cys-95, and the C-terminal 12 residues of the *Vibrio harveyi* ferric uptake regulator (Fur) are functionally inessential. *J. Microbiol.* 46, 670-680.

Thompson, C.C., F.L. Thompson, A.C. Vicente, and J. Swings. 2007. Phylogenetic analysis of vibrios and related species by means of *atpA* gene sequences. *Int. J. Syst. Evol. Microbiol.* 57, 2480-2484.

Tiss, A., O. Barre, I. Michaud-Soret, and E. Forest. 2005. Characterization of the DNA-binding site in the ferric uptake regulator protein from *Escherichia coli* by UV crosslinking and mass spectrometry. *FEBS Lett.* 579, 5454-5460.

Zhou, D., L. Qin, Y. Han, J. Qiu, Z. Chen, B. Li, Y. Song, and *et al*. 2006. Global analysis of iron assimilation and fur regulation in *Yersinia pestis*. *FEMS Microbiol. Lett.* 258, 9-17.